Desalination and Water Treatment
www.deswater.com

doi: 10.1080/19443994.2013.781966

51 (2013) 7639–7654
December

Taylor & Francis
Taylor & Francis Group

Adsorption performance of activated carbon prepared from elephant (*Elephas maximus*) dung for the removal of Reactive Yellow 15 from aqueous solution

C. Theivarasu[a,*], S. Chandra[b]

[a]*Department of Basic Sciences-Chemistry, PSG College of Technology, Peelamedu, Coimbatore 641004, India*
Tel. +91 9443577832; email: theivarasu@yahoo.co.in
[b]*Department of Chemistry and Applied Chemistry, PSG Polytechnic College, Coimbatore 641004, India*

ABSTRACT

Elephant Dung Activated Carbon (EDAC), prepared by acid treatment, was used as an eco friendly adsorbent for the removal of the textile dye, Reactive Yellow 15 (RY15) from an aqueous solution. Batch adsorption experiments were carried out to investigate the kinetic, thermodynamic and isotherm studies by varying the initial dye concentration and temperature. The adsorption kinetic data were correlated with pseudo first-order, pseudo second-order, and elovich models. Pseudo second-order kinetic model fitted very well with the experimental data. The thermodynamic parameters like Gibb's Free energy change (ΔG^0), Entropy change (ΔS^0), and enthalpy change (ΔH^0) were calculated. The results indicated that RY15 adsorption process was endothermic and spontaneous. The mechanism of adsorption process was determined by studying the intraparticle diffusion and liquid film diffusion models. Effects of EDAC dosage and pH on percentage removal of RY15 were studied. Maximum adsorption had taken place at pH 2. The experimental data were correlated with Langmuir, Freundlich, and Temkin adsorption isotherm models and it was best represented by Langmuir isotherm model. Adsorption capacity of EDAC was compared with different adsorbent/adsorbate systems. Desorption studies indicated the physisorption type of adsorption of RY15 onto EDAC. The effectiveness of the adsorbent was tested with an effluent collected from a dyeing industry. Competitive adsorption of various types of dyes was examined to study the performance of EDAC.

Keywords: Elephant dung; Reactive Yellow 15; Adsorption; Kinetics; Thermodynamics; Isotherm

1. Introduction

Textile and dyeing industry effluents can create serious environmental pollution problems when they are discharged into water bodies. The untreated effluents possess toxic dyes and pigments which impart color even at low concentration. These hazardous materials affect photosynthetic activity [1] because of reduced light penetration. So it is important to adopt some treatment methods before discharging the effluents into water to reduce the harmful effects. The methods employed for the removal of dyes from wastewaters include anaerobic decolorization [2], chemical oxidation [3], reverse osmosis [4], ion exchange [5] and biological treatment [6]. These physico chemical methods are less efficient, expensive

---

*Corresponding author.

1944-3994/1944-3986 © 2013 Balaban Desalination Publications. All rights reserved.

and produce wastes that are difficult to dispose. Among these methods, adsorption [7] onto activated carbon has been proven to be the most effective method for the color removal in terms of initial cost, simplicity of design, easy operation and insensitivity to toxic substances [8]. Adsorption process is more advantageous than the other conventional methods due to its sludge-free clean process and high adsorption capacity for the colored particles. However, usage of commercial activated carbon for adsorption has some limitations like high cost and regeneration problems. This has necessitated the exploration of some effective, cheaper and easily available alternatives. Such alternatives include low-cost activated carbons prepared from natural products like date pits [9], bagasse [10], fruit stones and nutshells [11], jute fiber [12], rice husks [13], plum kernels [14], and coconut shells [15]. Activated carbons prepared from various products are widely used as adsorbents due to their high adsorption capacity, large surface area and micro porous structure. The wide usefulness of activated carbon as adsorbent is a result of their chemical and thermal stability. In this study, an attempt has been made to utilize activated carbon prepared from elephant dung for the removal of RY15 from aqueous solution. Elephant dung is available in large quantities throughout the year in the western districts of Tamil Nadu and Kerala, a nearby state. Further, the zero or negligible cost of elephant dung makes this project feasible and cost effective for the removal of RY15, a reactive dye from aqueous solution. Reactive Yellow 15 is a water-soluble dye used for dyeing cellulose fibers like cotton, viscose, and rayon. Large fractions of reactive dyes (10–50%) are wasted during the dyeing process, up to 0.6–0.8 g/dm^3 is detected in dye house effluent [16].

The main objectives of the study are the following: Evaluating the possibility of using elephant dung as a low-cost activated carbon and studying its application to remove RY15 from wastewater through batch adsorption experiments; Studying the adsorption mechanism through kinetic and equilibrium data; determining the thermodynamic and adsorption isotherm parameters.

2. Materials and methods

2.1. Adsorbate

Reactive Yellow 15 (CAS No.: 12226-47-0; Molecular formula: $C_{20}H_{20}N_4Na_2O_{11}S_3$; Molar Mass: 634.5; λ_{max}: 420 nm) was procured from Sigma Aldrich and used as received without further purification. A stock solution of the dye (1,000 mg/L) was prepared by dissolving the dye in distilled water. Dilutions of required initial concentrations (10, 20, 30, and 40 mg/L) were made. The UV spectrum of RY15 is presented in Fig. 1.

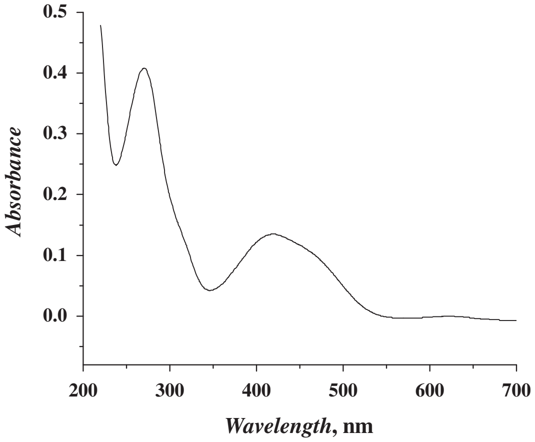

Fig. 1. UV spectrum of RY15.

2.2. Adsorbent

Elephant dung was collected and air-dried. The lumps of the dung were then crushed. The crushed elephant dung was activated using concentrated sulfuric acid (1:2) in a hot air oven at 120˚C for 3 h. The acid was then removed by repeated washings with a large quantity of distilled water. It was then dried in a hot air oven for 6 h. The carbon was then ground, sieved (<150 μ), and stored in air tight container. It was then used as Elephant Dung Activated Carbon (EDAC) for batch adsorption experiments [17].

2.3. Determination of surface area

The surface area of EDAC was determined using N_2-desorption quantachrome Nova 1200 e BET surface area analyzer.

2.4. Batch adsorption experiments

Batch adsorption experiments were conducted to study the effect of contact time, chemical kinetics, the effect of temperature, the effect of adsorbent dosage, the effect of pH, and isotherms. Batch adsorption experiments were carried out at room temperature by taking different initial dye concentrations (10, 20, 30, and 40 mg/L). 50 mL of the dye solution was taken in 250 mL conical flasks with desired dosage of EDAC. The conical flasks were then shaken using Labline shaking incubator at a constant agitation speed

(120 rpm). The samples were withdrawn from the shaker at predetermined time intervals, and the supernatant liquid portions were centrifuged using R-8C laboratory centrifuge (Remi make) at 2000 rpm for 20 min and analyzed for remaining dye concentration spectrophotometrically using Schimadzu UV-1700 PharmaSpec UV visible spectrophotometer.

The amount of dye adsorbed onto activated carbon was calculated as follows.

$$q_e = (C_0 - C_e)v/w \tag{1}$$

where C_0 and C_e are the initial and equilibrium concentrations (mg/L) of the dye solutions respectively. v is the volume of the dye solution taken and w is the weight of the adsorbent used.

2.5. Desorption studies

After adsorption experiments, the RY15 loaded EDAC was separated out by filtration using Whatman filter paper No. 42. The RY15 loaded EDAC was washed gently with double distilled water to remove the unadsorbed dyes if present. Desorption experiments were carried out by agitating RY15 loaded EDAC with 50 ml of neutral pH water, Sodium hydroxide(1 M), Sulfuric acid (1 M) and 50% acetic acid (v/v). The desorbed dye solutions were separated by centrifugation and estimated.

2.6. Analysis of textile industry effluent

An effluent was collected from a dyeing unit Tirupur, Tamil Nadu, India after primary treatment. It was then diluted and assessed for its physico-chemical and biological parameters like chloride, pH, conductivity, total dissolved solids (TDS), alkalinity, Biochemical oxygen demand (BOD) and chemical oxygen demand (COD), as per the standard procedures described in APHA 1992 [18]. Alkalinity and TDS were determined by volumetric and gravimetric methods respectively. pH and conductivity were determined using pH meter (Systronix digital pH meter 335) and conductivity meter (Elico CM 180). BOD was determined at 20˚C for 5 days by dilution method and COD by closed refluxed method. Chloride content was determined by argentometric method. 50 ml of the effluent was shaken with one gram of EDAC for 3 h using Labline shaking incubator at a constant agitation speed (120 rpm). Then the adsorbent and the effluent were separated and analyzed as before.

2.7. Competitive adsorption

The adsorption spectra of mixture of 50 ml of Acid Blue 92 (AB92), Rhodamine B (RhB), Crystal Violet (CV), Malachite green (MG) and Reactive Yellow 15 (RY15) with a concentration of 20 mg/L of each dye was recorded spectrophotometrically. The mixture was then treated with 150 mg of EDAC for 2 h in a batch reactor at 120 rpm. The adsorbent was then separated and the supernatant liquid was analyzed spectrophotometrically as before.

3. Results and discussion

3.1. BET surface area analysis

BET surface area is determined by flowing nitrogen gas at 77 K through activated carbon sample and allowing the nitrogen to enter into the pores of the carbon. From the amount of nitrogen that has been absorbed into the pores, the surface area is deduced. A plot of relative pressure (P/P_o) vs. $1/[W\ ((P_o/p)-1)]$ gives the linear BET isotherm of EDAC. The BET surface area of EDAC was found to be 37.869 m^2/g, and the average pore volume of the adsorbent was determined as 0.08782 cc/g for the pores smaller than 137 nm (Diameter) at P/P_o.

3.2. Effect of initial concentration and time

Batch adsorption experiments were carried out to study the influence of contact time and initial dye concentration on the distribution of the dye between the adsorbent and the dye solution at equilibrium. It is also important to assess the adsorption capacity of the adsorbent for the adsorbates. It was found that the adsorption was rapid in the initial stages, gradually increased and reached equilibrium after a particular time. This could be due to the fact that, in the initial stages of adsorption process, the dye molecules reach boundary layer, diffuse into the adsorbent surface and finally into the pores of the adsorbent. As so many dye molecules adsorbed initially, the number of unoccupied sites decreased and the adsorbent surface approaches saturation. Similar results were reported in the literature using low-cost adsorbents [19,20]. The equilibrium time was found to be 240 min for 40 mg/L, 210 min for 30 mg/L, 180 min for 20 mg/L and 150 min for 10 mg/L, respectively. Further, the amount of dye adsorbed increased with an increase in initial dye concentration. This is because increase in initial concentration enhanced the driving force between the aqueous and solid phases and increased number of collisions between dye molecules and the adsorbent [21]. From the data obtained, it was also understood that the adsorption was dependent on initial dye concentration. The data also revealed that the percent removal of dyes decreased with increase in the dye concentration suggesting that dye removal by adsorption was concentration dependent due to the saturation of adsorption sites on the adsorbent surface. The reason is that, at low concentrations, the ratio of the number of molecules to the available surface area is low. Subsequently, the fractional adsorption becomes independent of initial concentration. However, at high concentrations, the available sites of adsorption become fewer, and hence, the percentage removal of the dye was dependent on initial dye concentration [22].

3.3. Adsorption kinetics

The chemical kinetics describes reaction pathways along time to reach equilibrium, whereas chemical equilibrium does not give any information about the pathways and rate of reaction. Adsorption kinetics is highly dependent on the physical and chemical characteristics of the adsorbent material. The adsorption of dyes from liquid to solid phase can be considered as a reversible reaction with equilibrium established between the two phases. The efficiency of process operation requires an understanding of the kinetics of uptake or the time dependence of the concentration distribution of the solute in both bulk solution and solid adsorbent. Kinetics of sorption also describes the solute uptake rate, which in turn governs the residence time of sorption reaction. It is one of the important characteristics in defining the efficiency of sorption. In order to investigate the mechanism of adsorption of RY15 onto EDAC three different kinetic models, namely, pseudo first-order, pseudo second-order and elovich models were applied to the experimental data.

3.3.1. Pseudo first-order kinetic model

This was the first equation for the adsorption of liquid/solid system based on the solid capacity [23]. This model was described as follows [24].

$$dq_t/d_t = k_1(q_e - q_t) \tag{2}$$

where q_e and q_t are the amount adsorbed (mg/g) at equilibrium and at time, t, respectively, and k_1 is the pseudo first-order rate constant (min^{-1}). After integration by applying conditions, $q_t = 0$ at $t = 0$ and $q_t = q_t$ at $t = t$, then the equation becomes,,

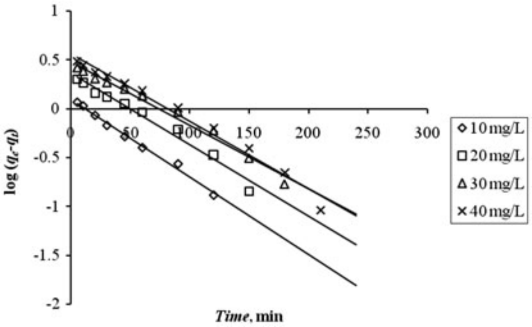

Fig. 2. Pseudo first order kinetic model.

$$\log(q_e - q_t) = \log q_e - (k_1/2.303)t \tag{3}$$

A plot (Fig. 2) of log (q_e−q_t) vs. time for various initial concentrations (10, 20, 30, and 40 mg/L) gives linear lines. The values of k_1 and q_e were calculated from the slope and intercept of the plot, respectively. The correlation coefficient of pseudo first-order kinetic model obtained for all initial concentrations are relatively low. This indicates that the sorption of RY15 does not follow pseudo first-order kinetics. The inapplicability of the Lagergren equation to describe the kinetics of dyes sorption was also observed for adsorption of dyes using banana and orange peels [5].

3.3.2. Pseudo second-order kinetic model

Kinetic data were further treated with pseudo second-order kinetic model. Pseudo second-order equation is based on the sorption capacity of the solid phase [25]. The differential equation is given as follows.

$$dq_t/dt = k_2(q_e - q_t)^2 \tag{4}$$

where q_e and q_t are the adsorption capacity at equilibrium and time t, respectively, (mg/g) and k_2 is the rate constant of pseudo second-order adsorption (g/mg min). Integration of the above equation for the boundary conditions $t = 0$ to $t = t$ and $q = 0$ to q_e gives

$$1/(q_e - q_t) = 1/q_e + k_2 t \tag{5}$$

The above equation is the integrated law for a pseudo second-order reaction. The above equation can be rearranged to obtain

$$t/q_t = 1/k_2 q_e^2 + (1/q_e)t \tag{6}$$

A plot (Fig. 3) of t/q_t vs. t gives a linear relationship which proves that the adsorption follows Pseudo

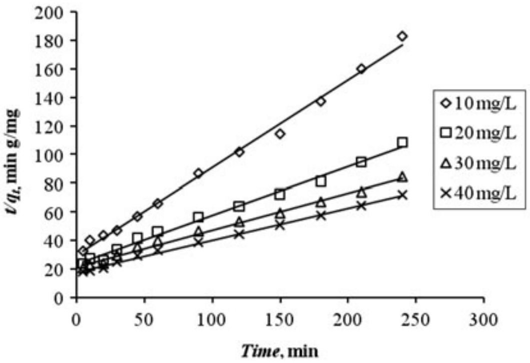

Fig. 3. Pseudo second order kinetic model.

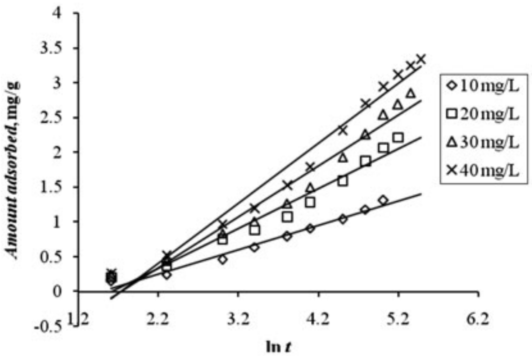

Fig. 4. Elovich model.

Table 1
Kinetic parameters

Concentration (mg/L)	10	20	30	40
Pseudo first order kinetic model				
$q_{e.exp}$ (mg/g)	1.314	2.214	2.835	3.345
$q_{e.cal}$ (mg/g)	1.631	2.924	3.891	4.464
$k_1 \times 10^{-2}(\text{min}^{-1})$	1.612	1.612	1.381	1.381
r^2	0.992	0.975	0.983	0.981
SSE	0.362	0.691	0.534	0.711
Pseudo second order kinetic model				
$q_{e.cal}$ (mg/g)	1.230	2.280	5.260	5.915
$k_2 \times 10^{-3}$(g/mg min)	9.678	5.009	3.092	2.822
r^2	0.995	0.992	0.992	0.996
SSE	0.398	0.293	0.560	0.478
Elovich model				
α (mg/g min)	0.103	0.113	0.129	0.154
β (g/mg)	2.857	1.742	1.367	1.161
r^2	0.980	0.962	0.955	0.968

second-order kinetics. q_e and k_2 were calculated from the slope and intercept of the plot respectively. The equilibrium sorption capacity q_e, is increasing while increasing the initial dye concentration but a decreasing trend was observed in the pseudo second-order rate constant k_2. Moreover, the calculated values of equilibrium adsorption capacity q_e for all the initial dye concentrations were in good agreement with the experimental data. It was also observed that the correlation coefficient r^2 values are higher than pseudo first-order r^2 values. From the results, it was understood that pseudo second-order kinetics describes the adsorption of RY15 onto EDAC much better than pseudo first-order kinetic model.

3.3.3. Elovich model

Elovich equation is mainly used to describe the second order kinetics assuming that the actual solid surfaces are energetically heterogeneous [26]. Elovich model is generally expressed as follows [27].

$$\mathrm{d}q_t/\mathrm{d}_t = \alpha e^{-\beta qt} \tag{7}$$

where α and β are constants. The constant "α" is considered as the initial rate because $(\mathrm{d}q_t/\mathrm{d}_t) \to \alpha$ as $q_t \to 0$. Given that $q_t = 0$ at $t = 0$ and "β" is an indication of the number of sites available for adsorption. The integrated form of the above equation is as follows.

$$q_t = (1/\beta)\ln(t + t_0) - (1/\beta)\ln t_0 \tag{8}$$

where $t_0 = (1/\alpha\ \beta)$. If $t >> t_0$, it is simplified as

$$q_t = (1/\beta)\ln(\alpha\beta) + (1/\beta)\ln t \tag{9}$$

The parameters α and β were calculated from the slope and intercept of the plot (Fig. 4) of ln*t* vs. time, respectively. Lowering of β values with increase in initial dye concentrations and justification of $t >> t_0$ predict the behavior adsorption of dyes over the whole range of variables studied, strongly supports the validity of Elovich equation. The initial adsorption rates, α, increases while increasing the initial concentration from 10 to 40 mg/L. Kinetic parameters of pseudo first-order, pseudo second-order and Elovich models are listed in Table 1.

Applicability of each kinetic model equation was tested with the sum of error squares (SSE) using the following formula [28].

$$\mathrm{SSE} = \sqrt{\Sigma(q_{e\cdot \exp} - q_{e\cdot \mathrm{cal}})^2/N} \tag{10}$$

where N is the number of data points. A kinetic model having higher r^2 values and lower SSE values will have a best fit with the experimental data. In this study, pseudo second-order kinetic model r^2 values are closer to unity and the SSE values are lower. This proves that pseudo second-order kinetic model provides a good correlation for the adsorption of RY15 onto EDAC. Similar reports have already been recorded for the adsorption of Methylene Blue onto bamboo-based activated carbon [29]; Adsorption of direct dyes on activated carbon prepared from sawdust [30]; Adsorption of Congo red on activated carbon from coir pith [31].

3.4. Effect of temperature

Temperature plays an important role in the adsorption process of dyes. Increase in temperature, increases the rate of diffusion of the adsorbate molecules across the external boundary layer and into the internal pores of the adsorbent, due to the decrease in viscosity of solution. The effect of temperature on the adsorption of RY15 was examined by carrying out experiments at 301, 308, 318, 328, and 338 K with 50 ml of 40 mg/L dye solution with 250 mg adsorbent. From the results, it was observed that the percentage removal of the dye increased as the temperature increased. Increase in dye uptake with increase in temperature revealed that the adsorption of dyes onto EDAC was endothermic in nature. When the temperature is increased, the mobility of the dye molecules increased and the retarding forces on the diffusing ions decreased, thereby increasing the sorption capacity of the adsorbent [32]. The enhancement of adsorption capacity of the adsorbent at high temperatures was also attributed to the enlargement of pore size and activation of the adsorbent surface [33]. Equilibrium time of 40 mg/L of RY15 was reduced from 240 to 210 min. This is due to the reason that, increase in temperature, increases the particle density, which form voids, resulting in a reduced equilibrium time [34]. Similar results were reported by Sreelatha et al. [35] and Ncibi et al. [36] for the adsorption of reactive dyes (Reactive Red 141 and Reactive Blue 21) using palm shell powder (An Agrowaste) and chitosan as adsorbents and for the adsorption of textile reactive dye (Reactive Red 228) using *Posidonia oceanica* (L.) fibrous biomass as an adsorbent, respectively. From the results, it was understood that increase in temperature increases the adsorption capacity of the adsorbent indicating that adsorption of dyes onto EDAC is highly dependent on temperature.

3.5. Evaluation of thermodynamic parameters

In order to fully understand the nature of adsorption, it is important to determine the thermodynamic parameters such as Gibb's free energy change (ΔG^0), enthalpy change (ΔH^0) and entropy change (ΔS^0). Based on fundamental thermodynamics concept, it is assumed that in an isolated system, energy cannot be neither gained nor lost and the entropy change is the only driving force. In environmental engineering practice, both energy and entropy factors must be considered in order to determine the spontaneity of the process. The Gibb's free energy change (ΔG^0) is the fundamental criterion of spontaneity. Reactions occur spontaneously at a given temperature, if (ΔG^0) is negative. If the change in entropy ΔS^0 is positive, the degree of disorder was increased by the adsorption reaction. Positive ΔH^0 values suggested the endothermic nature of adsorption.

Gibb's free energy change (ΔG^0), change in enthalpy (ΔH^0), and change in entropy (ΔS^0) were determined from adsorption affinity parameter, K_c, which is the ratio of the amount of dye adsorbed per unit mass C_{ad} to the equilibrium concentration C_e of the adsorbate. The value of K_c is obtained from the following equation.

$$K_c = q_e/C_e \tag{11}$$

where q_e is the concentration of the dye in solid phase and C_e is the concentration of the dye in solution phase. The Gibb's free energy change (ΔG^0) is calculated as follows.

$$\Delta G^0 = \Delta H^0 - T\Delta S^0 \tag{12}$$

The equation can also be written as

$$\ln K_c = \Delta S^0/R - \Delta H^0/RT \tag{13}$$

The Van't Hoff plot ($\ln K_c$ vs. $1/T$) of RY15 is presented in Fig. 5 and the thermodynamic parameters evaluated are listed in Table 2. It was observed from the results that ΔG^0 values obtained were negative which confirmed that the adsorption of RY15 onto

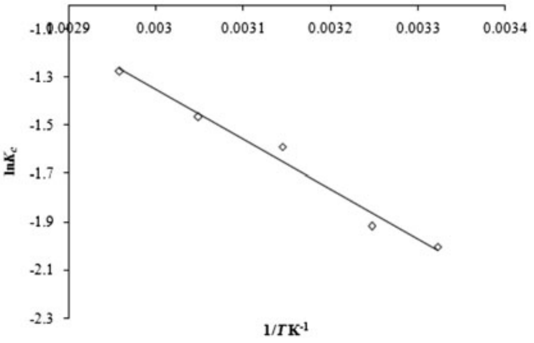

Fig. 5. Van't Hoff plot.

Table 2
Thermo dynamic parameters

Temperature (K)	301	308	318	328	338
$-\Delta G$ (kJ mol^{-1})	29.308	29.591	29.994	30.397	30.800
ΔH (kJ mol^{-1}) = 17.176		ΔS (J K^{-1} mol^{-1}) = 40.306			
E_a (kJ mol^{-1}) = 18.498					

EDAC was spontaneous. It was also found that the ΔG^0 values decreased from −29.308 to −30.80 kJ mol^{-1}. This proved that the adsorption process was feasible and spontaneous [37]. The positive values of ΔH^0 (17.176 kJ mol^{-1}) confirmed the endothermic nature adsorption [38]. The positive values of ΔS^0 (40.306 J K^{-1}mol^{-1}) proved the increased randomness at the solid solution interface during adsorption process [39]. When the dye molecules get adsorbed on the adsorbent surface, water molecules previously bonded to the surface get released and dispersed in the solution resulting in an increase in entropy. This is due to the reason that the previously adsorbed water molecules, which are displaced by the adsorbate species, gain more transitional entropy than is lost by the adsorbate molecules thus allowing the prevalence of randomness in the system [40].

3.6. *Activation energy*

Activation energy is an important parameter in thermodynamic studies because it determines the temperature dependence of the reaction rate. In adsorption process, activation energy is defined as the energy that must be overcome by the adsorbate ion/molecule to react/interact with the functional groups on the surface of the adsorbent. It is the minimum energy required for a specific adsorbate–adsorbent interaction to occur. The activation energy (E_a) for the adsorption of an adsorbate ion/molecule onto an adsorbent surface in an adsorption process can be determined from experimental measurements of the adsorption rate constant at different temperatures according to the Arrhenius relation that is given as

$$K = Ae^{-Ea/RT} \tag{14}$$

Linear form of the above equation is as follows

$$\ln k_2 = \ln A - E_a/RT \tag{15}$$

where k_2 is the pseudo second-order rate constant (g/mg min), A is a constant called the frequency factor, E_a is the activation energy (kJ mol^{-1}), R is the universal gas constant (8.314 J K^{-1} mol^{-1}), and T is the absolute temperature (K). By plotting lnk_2 vs. $1/T$, values of E_a and A can be obtained from the slope and the intercept of the plot (Fig. 6), respectively [41].

The magnitude of the activation energy gives an idea about the type of adsorption. Two main types of adsorptions are physical and chemical adsorption. Low activation energies (5–40 kJ mol^{-1}) are characteristics of physical adsorption, while higher activation energies (40–800 kJ mol^{-1}) suggest chemical adsorption [42]. In this study, the energy of activation of RY15 is found to be 18.498 kJ mol^{-1} indicating the physisorption mechanism.

3.7. *Mass transfer studies*

It is important to predict the mechanism of adsorption for the designing of batch adsorber [43]. The mechanism of adsorption of a sorbate on a sorbent follows a series of steps. The slowest of these steps controls the overall rate of the adsorption process. Generally, pore and intraparticle diffusion are often rate limiting in a batch reactor and film diffusion is more likely rate limiting in a continuous flow system [44]. In this study, both intra particle diffusion and liquid film diffusion models were studied.

3.7.1. *Intraparticle diffusion model*

For a solid/liquid adsorption process, the transfer of solute is characterized by external mass transfer (boundary layer diffusion) or internal diffusion or both. The rate-controlling parameter might be

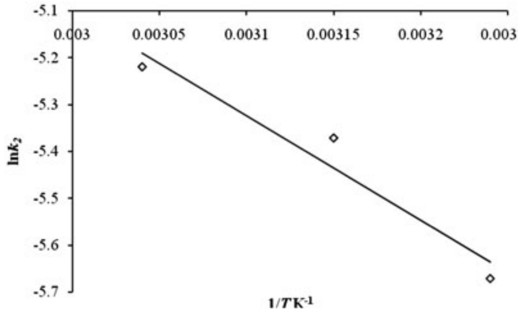

Fig. 6. Arrhenius plot.

distributed between intraparticle and film diffusion mechanism. Whatever the case external diffusion will be involved in the sorption process. An intraparticle diffusion coefficient K_{id} is given by the following equation [45].

$$q_t = K_{\mathrm{id}} t^{1/2} + C \tag{16}$$

The plot (q_{t} vs. $t^{1/2)}$ of intraparticle diffusion of RY15 for different initial dye concentrations (10, 20, 30 and 40 mg/L) is shown in Fig. 7. The figure shows that there are three different stages of adsorption. The initial curved portion is due to the boundary layer diffusion (film diffusion), the second linear portion represents the intraparticle diffusion and the third portion is the equilibrium stage where intraparticle diffusion starts to slow down and there is no significant adsorption taking place. The slope of the second linear portion of the plot q_{t} vs. $t^{1/2}$ has been defined to yield the intraparticle diffusion parameter K_{id} (mg/g/min$^{1/2}$). On the other hand, intercept of the plot represents the boundary layer effect. The larger the intercept, greater the contribution of surface adsorption in the rate controlling step. The rate constants of intraparticle diffusion mechanism are found to increase with increase in initial concentration of the dye. If the intraparticle diffusion is the only rate-limiting step, then the lines would pass through the origin; if not, the boundary layer diffusion also controlling the adsorption to some extent. It could be observed from the figures that the lines did not pass through the origin indicating that intraparticle diffusion was not the only rate-limiting step [46].

3.7.2. Liquid film diffusion model

When the transport of the solute molecules from the liquid phase to the solid phase, boundary layer plays an important role in adsorption process [47]. The liquid film diffusion model is represented as follows.

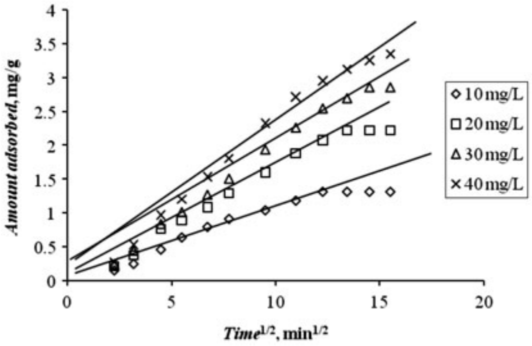

Fig. 7. Intraparticle diffusion model.

$$\ln(1 - F) = k_{\mathrm{fd}} t \tag{17}$$

where F is the fractional attainment of equilibrium and k_{fd} is the liquid film diffusion rate constant (min^{-1}). A linear plot of-ln(1−F) vs. time, t would suggest that the kinetics of the adsorption process is controlled by diffusion through the liquid film surrounding the solid adsorbent [48]. The plot of film diffusion of RY15 for different initial dye concentrations (10, 20, 30, and 40 mg/L) is shown in Fig. 8. The values of k_{fd} were calculated from the slopes of the respective linear lines of the plot. The intraparticle and liquid film diffusion parameters are presented in Table 3. It is suggested from the results that the adsorption process may also be controlled by liquid film diffusion. However, the intercept was not close to zero, indicating indubitable contribution to the rate from particle diffusion [49].

3.7.3. Mechanism of adsorption

Mechanism of sorption is either film diffusion controlled or particle diffusion controlled [50]. Generally, three types of mechanisms are involved in the sorption process, mentioned as follows [51]:

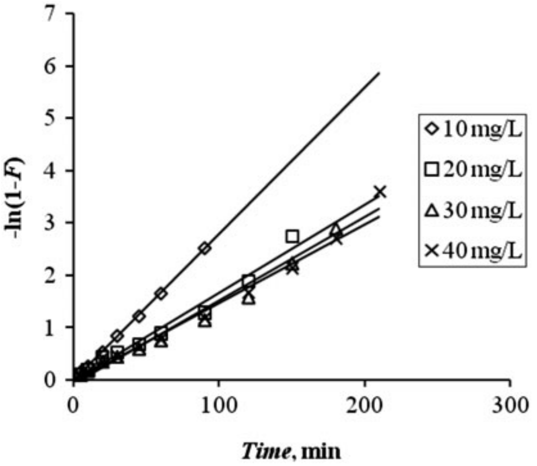

Fig. 8. Liquid film diffusion model.

Table 3
Intraparticle and liquid film diffusion parameters

Concentration (mg/L)	10	20	30	40
Intra particle diffusion model				
k_{id} (g/mg min$^{1/2}$)	0.096	0.160	0.223	0.197
r^2	0.992	0.996	0.998	0.990
Liquid film diffusion model				
k_{fd} (g/mg min$^{1/2}$)	0.028	0.016	0.015	0.015
r^2	0.989	0.975	0.981	0.981

(1) Film diffusion, where the adsorbate ions travel toward the external surface of the adsorbent.
(2) Particle diffusion, where the adsorbate ions travel within the pores of the adsorbent excluding a small amount of adsorption that occurs on the exterior surface of the adsorbent.
(3) Adsorption of the adsorbate ions on the interior surface of the adsorbent.

In order to predict the actual slow step involved in the adsorption process, the kinetic data were further analyzed using Boyd model which is given as follows [47].

$$F = 1 - 6/\Pi^2 \exp(-B_t) \quad (18)$$

where B_t is a mathematical function of F and F is the fractional attainment of equilibrium at time t. F is calculated using the following equation

$$F = q_t/q_e \quad (19)$$

where q_t and q_e are the amounts adsorbed (mg/g) at time t and at equilibrium, respectively. Rearranging the Eq. (19)

$$1 - F = 6/\Pi^2 \exp(-B_t) \quad (20)$$

or

$$B_t = -0.4977 - \ln(1 - F) \quad (21)$$

The above equation is used to calculate the B_t values at different time t. The linearity of the plot, B_t vs. t is used to determine whether the sorption process is film diffusion controlled or intra particle diffusion controlled. The plot of B_t vs. t of RY15 is shown in Fig. 9, and the results are presented in Table 3. For film diffusion to occur, the lines should pass through the origin. It was observed from the results that the lines do not pass through the origin indicating that film diffusion alone is not rate limiting. So it can be concluded that both intraparticle diffusion and film diffusion control the adsorption process. It can also be concluded that intraparticle diffusion has more control over the adsorption process due to the reason that the low linearity of the film diffusion model indicating a very low applicability of the model.

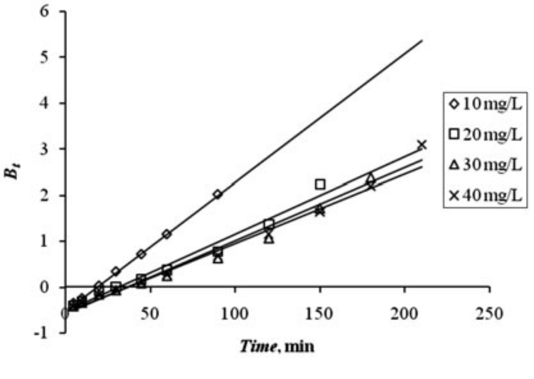

Fig. 9. Boyd's plot.

3.8. Effect of adsorbent dosage

Effect of adsorbent dosage plays an important role in standardizing the adsorption process. It is an important parameter in determining the capacity of adsorbent for initial concentration of adsorbate. Studying the effect of adsorbent dose gives an idea of the effectiveness of an adsorbent and the ability of a dye to be adsorbed with a minimum dosage of the adsorbent. To explain the effect of adsorbent dose on adsorption of RY15 onto EDAC, experiments were conducted by varying the adsorbent doses from 10 to 250 mg with 50 ml of different initial dye concentrations (10, 20, 30, and 40 mg/L) at room temperature. The optimum dosage of EDAC for the removal of RY15 was found to be 250 mg. It was clear from the results that percentage removal of RY15 increases with increase in the dosage of EDAC and reaches saturation after a particular amount of EDAC. This is due to the fact that, increase in adsorbent dose, increases the number of adsorption sites on the surface of the adsorbent [32]. Beyond the optimum dosage of the adsorbent, there is no significant increase in adsorption. This is because the amount of ions bound to the adsorbent and the amount of free ions remains constant even after the addition of optimum dosage of the adsorbent. It is obvious that increase in adsorbent dose increases the removal efficiency of EDAC, but the percent removal decreases with increase in initial dye concentrations from 10 to 40 mg/L. This was due to the reason that adsorption sites remain unsaturated during the adsorption process [52]. The increase in percent removal was also due to conglomeration of carbon at higher dosages [53].

3.9. Effect of pH

It is important to study the effect of pH of EDAC on adsorption of dyes because; pH is one of the key factors controlling the adsorption process. All carbons acquire different types of surface charges according to their functional groups present on the surface of the adsorbent. The interactions with H^+ and OH^- ions can show amphoteric properties of the carbon surface. Change of pH affects the adsorption process through dissociation of functional groups on the adsorbent

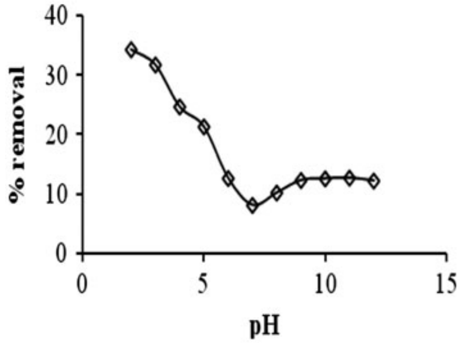

Fig. 10. Effect of pH on percentage removal of RY15.

surface active sites. This leads to a change in reaction kinetics and equilibrium characteristics of the adsorption process. Dissolution of dyes release colored dye ions into solution. Adsorption of these ions onto adsorbent surface is primarily influenced by the surface charge of the adsorbent, which in turn influenced by the solution pH. Hence adsorption is mainly dependent on the nature of the dye species and surface charge on the adsorbent.

Effect of percentage removal of RY15 by EDAC is represented in Fig. 10. The percent removal of RY15 decreased from 34.33 to 12.73% when the dye solution pH was increased from 2 to 11. Maximum removal (34.33%) was observed at pH 2. The results showed that higher percent removal took place at highly acidic medium and basic solution pH did not favor the adsorption of RY15 by EDAC. Generally, reactive dyes ionize to a high degree in aqueous solutions to form coloured anions due to the presence of sulfonate groups in their structures. The sulfonate groups are easily dissociated and have negative charges in the aqueous medium. As the pH of the solution decreased, the protonated surface groups facilitated the sorption of negatively charged dye molecules [54], thereby increasing the percentage removal of RY15 by EDAC. Similar reports have already been found in the literature for the adsorption of reactive Orange 16 using *Corynebacterium glutamicum* as a low-cost biosorbent by Won et al. [55] and for the adsorption of Reactive Red 195 using chitosan by Yue-zhong et al. [56].

3.10. Adsorption isotherm

Adsorption isotherm models are widely used to describe the adsorption progress and to investigate the mechanism of adsorption. The adsorption isotherm models are also fundamental in describing the interactive behavior between adsorbate and adsorbent. Analysis of isotherm data is important for predicting the adsorption capacity of the adsorbent, which is one of the main parameters required for the design of adsorption system. Isotherm models are also critical in optimizing the utility of the adsorbent [57]. Moreover, adsorption isotherm models clearly depict the relationship of amount adsorbed by unit weight of adsorbent with the concentration of adsorbent remaining in the medium at equilibrium. Thus, the correlation of equilibrium data using either a theoretical or empirical equation is essential for adsorption data interpretation and prediction. The correct interpretation of experimental adsorption isotherm can be realized in terms of some mathematical equations called adsorption isotherm model equations. In this regard, various isotherm equations have been used to describe the equilibrium nature of adsorption. Some of these selected models to describe the equilibrium characteristics of adsorption of RY15 onto EDAC are Langmuir, Freundlich and Temkin isotherm models. The applicability of the isotherm models to the adsorption study was compared by judging the correlation co efficient, r^2 values.

3.10.1. Langmuir isotherm

Langmuir isotherm has been widely used to describe the single solute system. Langmuir theory is based on an assumption that adsorption is a type of chemical combination or a process, and the adsorbed layer was unimolecular and intermolecular forces decreases rapidly with distance and consequently it predicts monolayer coverage of the adsorbent [58]. This isotherm assumes that adsorption takes place at specific homogeneous sites within the adsorbent and there is no significant interaction among the adsorbed species. This model further assumes uniform energies of adsorbate in the plane of the surface [59]. Theoretically, the adsorbent has a finite capacity for the adsorbate. Once a dye molecule occupies a site, further adsorption cannot take place at that site suggesting monolayer coverage of dyes. This indicates that the adsorption occurs until a monolayer of adsorption and after completion of adsorption no more interaction between the adsorbent and adsorbate molecules takes place [60]. The saturated monolayer capacity can be represented by the following expression.

$$q_e = b_L Q_0 C_e / 1 + Q_0 C_e \tag{22}$$

The linear form of equation is given as

$$C_e / q_e = 1 / b_L Q_0 + C_e / Q_0 \tag{23}$$

where C_e is the equilibrium concentration of dye (mg/L), q_e is the amount of dye adsorbed at equilibrium (mg/g), Q_0 is Langmuir constant related to maximum adsorption capacity (mg/g), b_L is Langmuir constant related to energy of adsorption (L/mg). The Langmuir constants Q_0 and b_L are calculated from the linear plot of C_e/q_e vs. C_e which is shown in Fig. 11. The value of adsorption capacity Q_0 of RY15 is found to be 16.129 mg/g. Values of Langmuir adsorption capacity of some low cost activated carbons are listed in Table 4.

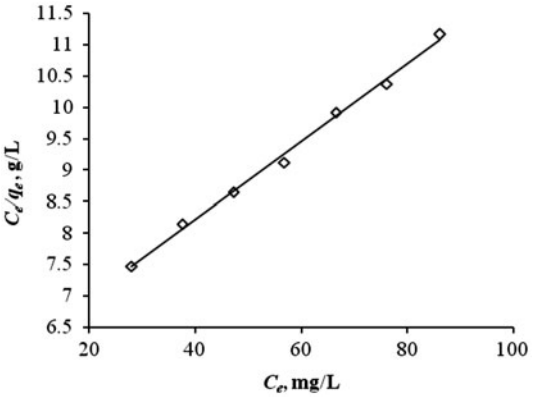

Fig. 11. Langmuir isotherm.

The essential feature of Langmuir isotherm can be expressed in terms of a dimensionless separation factor (R_L), given by the following equation

$$R_L = 1/(1 + b_L C_0) \tag{24}$$

where C_0 is the initial dye concentration (mg/L). R_L indicates the type of isotherm to be either unfavorable ($R_L > 1$), linear ($R_L = 1$), favorable ($0 < R_L < 1$) or irreversible ($R_L = 0$). In this study, the R_L values found to lie between 0 and 1, hence suggesting a favorable adsorption of RY15 onto EDAC.

3.10.2. Freundlich isotherm

Freundlich isotherm describes equilibrium on heterogeneous surfaces and hence does not assume monolayer capacity [73]. Freundlich model is based on the assumption that adsorption occurs on a heterogeneous adsorption surface having unequally available sites with different energies of adsorption [74]. Freundlich adsorption isotherm was originally empirical in nature but was later interpreted as the sorption to heterogeneous surfaces or surfaces supporting sites with varying affinities. Moreover, Freundlich adsorption isotherm model stipulates that the ratio of solute adsorbed to the solute concentration

Table 4
Comparison of adsorption capacity of EDAC with various adsorbent-adsorbate systems

Name of the adsorbent	Name of the dye	Adsorption capacity (mg/g)	References
Saw dust	Acid Yellow 36	183.8	[30]
Rice husk	Acid Yellow 36	86.9	[30]
Rice bran	Acid Red 138	0.43	[61]
Calcined alunite	Acid Yellow 17	151.5	[62]
	Acid Blue 40	212.8	
Euphorbia antiquorum L. wood	Acid Blue 92	222.22	[63]
Sago waste	Rhodamine B	16.2	[64]
Orange peel	Rhodamine B	14.3	[5]
Banana peel	Rhodamine B	20.6	[5]
Parthenium carbon	Rhodamine B	18.52	[65]
Coir pith carbon	Rhodamine B	8.06	[1]
Dried banana bark carbon	Rhodamine B	40.16	[66]
Ricinus communis pericarp	Crystal Violet	106.95	[67]
Flyash	Crystal Violet	9.76	[68]
Dried *Pandanus* leaves	Malachite Green	9.737	[69]
Sewage sludge char	Reactive Red 198	25	[70]
Corynebacterium glutamicum	Reactive Orange 16	154.8	[55]
EDAC	Rhodamine B	34.48	[17]
	Malachite green	45.45	[71]
	Reactive orange 16	7.518	[72]
	Reactive Yellow 15	16.129	This study

is a function of the solution. The empirical model was shown to be consistent with an exponential distribution of active centers. This model is used to explain the present adsorption phenomenon and is represented by the following equation.

$$q_e = K_F C_e^{1/n} \tag{25}$$

The linearized form of the above equation is expressed as follows:

$$\ln q_e = \ln K_F + 1/n \ln C_e \tag{26}$$

where K_F is the Freundlich adsorption isotherm constant (1/g) related to the extent of adsorption and $1/n$ is related to the adsorption intensity, which varies with the heterogeneity of the material. The values of K_F and $1/n$ are obtained from the intercept and slope of the plot (Fig. 12) of logq_e vs. logC_e The strength of linear relationship can be expressed by the correlation coefficient, r^2 values. This model exhibited slightly inferior correlation coefficient value than Langmuir model. The slope $1/n$ ranging from 0 to 1 is a measure of adsorption intensity or surface heterogeneity, becoming more heterogeneous as its value gets closer to zero [59].

3.10.3. Temkin isotherm

Temkin isotherm assumes that the effects of heat of adsorption that decreases linearly with coverage of the adsorbent and adsorbate interactions [75]. It also assumes that adsorption is characterized by a uniform distribution of binding energies up to some maximum binding energy. The basic form of Temkin equation is as follows:

$$q_e = RT \ln(K_T C_e)/b_T \tag{27}$$

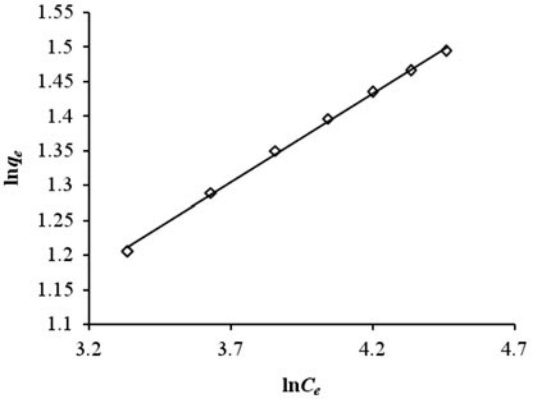

Fig. 12. Freundlich isotherm.

The linear form of Temkin euation is

$$q_e = RT \ln K_T/b_T + RT \ln C_e/b_T \tag{28}$$

where K_T is the equilibrium binding constant (L/g) of Temkin isotherm, b_T is the Temkin isotherm constant (kJ mol^{-1}) related to heat of sorption, T is the absolute temperature (K), R is the universal gas constant (8.314 J K^{-1} mol^{-1}). Temkin isotherm is obtained by plotting q_e vs. $\ln C_e$ at room temperature. The Temkin plot of RY15 is presented in Fig. 13. The higher equilibrium binding constants K_T values obtained for the dye indicated a stronger interaction between the dye and the adsorbent surface. The Temkin isotherm of RY15 showed a higher regression coefficient (>0.9) indicating the linear dependence of adsorption heat at low or medium coverages. The linearity may be due to the repulsion between or adsorbate species or to intrinsic surface heterogeneity [76]. The parameters obtained from Langmuir, Freundlich and Temkin isotherms are summarized in Table 5.

3.11. Desorption studies

The mechanistic aspects of adsorption and possibility of recovery adsorbent were investigated by conducting desorption studies. Regeneration of the adsorbent may make the treatment process more economical. If neutral pH water could desorb the dye after adsorption, it is understood that the dye is attached to the adsorbent by weak bonds. If acid or alkaline solution could desorb the dye, then the adsorption takes place by ion-exchange mechanism. If organic acids like acetic acid could desorb the dye, it is understood that the dye is attached to the adsorbent by a strong interaction of the chemisorption type of adsorption [22]. Form the various desorbing reagents used, RY15 is better desorbed (more than 60%) by alkaline medium indicating the physisorption type of adsorption of RY15 onto EDAC.

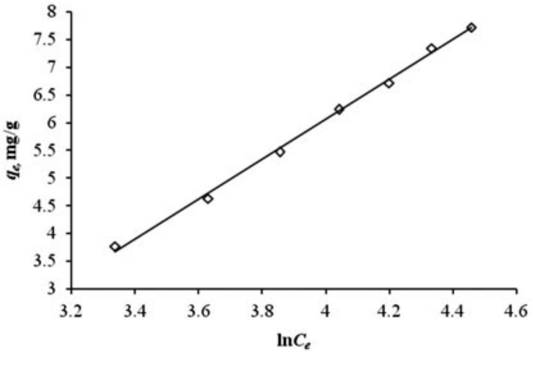

Fig. 13. Temkin isotherm.

Table 5
Isotherm parameters

Langmuir isotherm							
$b_L = 0.0108$			Q_m (mg/g) = 16.129		r^{2}=0.995		
C_o (mg/L)	60	80	100	120	140	160	180
R_L	0.606	0.536	0.479	0.435	0.397	0.365	0.339
Freundlich isotherm							
K_F (mg/g) = 1.42			$1/n = 0.257$		$r^2 = 0.998$		
Temkin isotherm							
k_T (L/g) = 0.098			b_T (kJ mol^{-1}) = 693.2		$r^2 = 0.997$		

Table 6
Characteristics of the dyeing industry effluent before and after treatment

Characterization		Untreated effluent	Treated effluent	WHO standards parameters[a]
1	pH	9.3	8.7	6.5–8.5
2	TDS (mg/L)	6,257	5,875	500–1,500
3	BOD (mg/L)	420	392	30
4	COD (mg/L)	3,250	2,746	250
5	Chloride (mg/L)	2,550	2,127	1,000
6	Alkalinity (mg/L)	1,496	1,230	NM[b]
7	Conductivity (μs/cm)	5,600	5,183	NM[b]

[a] Tolerance limits for the textile effluent discharged into inland water source as per World Health Organization Standards (WHO 1992).
[b] NM: Not mentioned.

3.12. Analysis of textile industry effluent

The physico chemical characteristics of untreated and treated forms of the textile industry effluent and World Health Organization Standards of drinking water (WHO 1992) are presented in Table 6. Untreated effluent was brownish black in color with high BOD, COD, and considerable amount of total alkalinity and chloride. The pH and conductivity of untreated effluent were high. High value of pH could be attributed to the presence of carbonates and bicarbonates [77]. The presence of high level of TDS might be due to the insoluble organic and inorganic matter present in the effluent [78]. High level of chloride was also responsible for the TDS. High chloride concentration was due to the addition of chloride salts in the bleaching and dyeing processes. High value of alkalinity was a result of the use of sodium carbonate as a scouring agent and caustic soda for the saponification of waxes, oils, and soils during fabric washing operations. High BOD of the effluent might be due to the presence of oxidizable organic matter present in the effluent [79]. Addition of various chemicals in different stages of dyeing operations was responsible for the higher level of COD in the effluent. The results show that almost all the parameters have higher values when compared to WHO standards.

Treatment with EDAC resulted in a slight decrease in the intensity of the color and the magnitude of the analyzed parameters for the treated effluent which are presented in Table 6.

3.13. Competitive adsorption of dyes

The competitive effect on decolorization of mixture of dyes before and after treatment with EDAC is

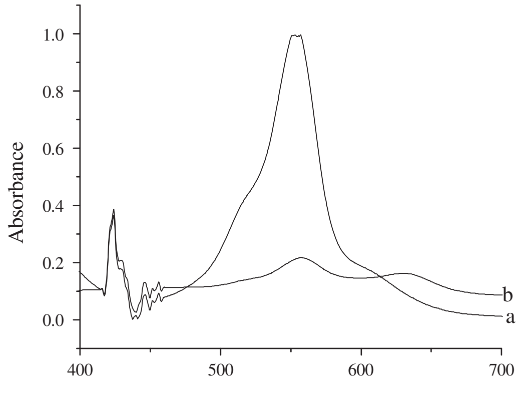

[a] UV Adsorption spectra of mixture of dyes before treatment
[b] UV Adsorption spectra of mixture of dyes after treatment

Fig. 14. UV spectra of competitive adsorption of dyes.

shown in Fig. 14. The $\lambda_{\max}$ of AB92, RhB, CV, MG and RY15 are 567, 556, 584, 617, and 420 nm, respectively. From the figure it was observed that the peaks of AB92, RhB, CV, and MG merged in the region between 500 and 650 nm. A peak is obtained at 424 nm corresponding to RY15. It was observed from the figure that the decolorization of acidic (AB92) and basic (RhB, CV, and MG) dyes was found to be around 90%. However, RY15, the reactive dye did not decolorize much. This is probably due to the predominant uptake of acidic and basic dyes. It may also be due to the competitive adsorption caused by the interaction between the dyes and to the changes of the adsorbent surface charge caused by the adsorption [80]. Different molecular weight, complexity and different functional groups of the dye structures are also responsible for the difference in color removal.

4. Conclusion

Sulfuric acid treated EDAC was used as an adsorbent for the removal of RY15 from aqueous solution by batch adsorption experiments. The equilibrium time was found to be 240 min for 40 mg/L, 210 min for 30 mg/L, 180 min for 20 mg/L, and 150 min for 10 mg/L dye solutions. The kinetics of adsorption process was investigated using Pseudo first order, Pseudo second order and Elovich models. The results showed that the adsorption process followed pseudo second-order kinetic model. Thermodynamic studies suggested that the adsorption process was spontaneous and endothermic in nature. Physisorption type of adsorption was confirmed by calculating the activation energy using Arrhenius equation. Mechanism of adsorption was explained by intraparticle and liquid film diffusion models. Percentage removal of RY15 increased by increasing the dosage of EDAC. Acidic solution pH favored the adsorption of RY15 by EDAC. The experimental data were better represented by Langmuir adsorption isotherm model compared to Freundlich and Temkin isotherm models. Desorption experiments indicated the physical nature of adsorption of RY15 onto EDAC. Moderate results were obtained by testing the applicability of EDAC on treating with a dyeing industry effluent.

References

[1] C. Namasivayam, R. Radhika, S. Suba, Uptake of dyes by a promising locally available agricultural solid waste: Coir pith, Waste Manage. 21(4) (2001) 381–387.

[2] R. Maas, S. Chaudhari, Adsorption and biological decolourisation of azo dye Reactive Red 2 in semicontinuous anaerobic reactors, Process Biochem. 40(2) (2005) 699–705.

[3] M. Muthukumar, D. Sargunamani, N. Selvakumar, Statistical analysis of the effect of aromatic, azo and sulphonic acid groups on discolouration of acid dye effluents using advanced oxidation processes, Dyes Pigm. 65(2) (2005) 151–158.

[4] N.A. Bastaki, Removal of methyl orange and Na_2SO_4 salt from synthetic waste water using reverse osmosis, Chem. Eng. Process 43(2) (2004) 1561–1567.

[5] G. Annadurai, R.S. Juang, D.J. Lee, Use of cellulose-based wastes for adsorption of dyes from aqueous solutions, J. Hazard. Mater. 92(3) (2002) 263–274.

[6] M. Wafaa, A. El-Rahim, H. Moawad, Enhancing bioremoval of textile dyes by eight fungal strains from media supplemented with gelatin wastes and sucrose, J. Basic Microbiol. 43(5) (2003) 367–375.

[7] P.C. Vandevivere, R. Bianchi, W. Verstaete, Treatment and reuse of waste water from the textile wet- processing industry: review of emerging technologies, J. Chem. Technol. Biotechnol. 72(4) (1998) 289–302.

[8] O. Hamdaoui, Batch study of liquid–phase adsorption of methylene blue using cedar sawdust and crushed brick, J. Hazard. Mater. 135(1–3) (2006) 264–273.

[9] B.S. Girijis, A.A. El-Hendawy, Porosity development in activated carbons developed from date pits under chemical activation with phosphoric acid, Micropor. Mesopor. Mater. 52(3) (2002) 105–117.

[10] W.T. Tsai, C.Y. Chang, M.C. Lin, S.F. Chien, H.F. Sun, M.F. Hsieh, Adsorption of acid dye onto activated carbons prepared from agricultural waste bagasse by $ZnCl_2$ activation, Chemosphere 45(1) (2001) 51–58.

[11] A. Aygun, S. Yenisoy-Karakas, I. Duman, Production of granular activated carbon from fruit stones and nutshells and evaluation of their physical, chemical and adsorption properties, Micropor. Mesopor. Mater. 66(2–3) (2003) 189–195.

[12] S. Senthilkumar, P.R. Varadarajan, K. Porkodi, C.V. Subbhuraam, Adsorption of methylene blue onto jute fibre carbon: kinetic and equilibrium studies, J. Colloid Interf. Sci. 284 (1) (2005) 78–82.

[13] N. Yalcin, V. Sevinc, Studies of the surface area and porosity of activated carbons prepared from rice husks, Carbon 38(14) (2000) 1943–1945.

[14] F.C. Wu, R.L. Tseng, R.S. Juang, Pore structure and adsorption performance of the activated carbons prepared from plum kernels, J. Hazard. Mater. 69(3) (1999) 287–302.

[15] W. Su, L. Zhou, Y.P. Zhou, Preparation of micro porous activated carbon from coconut shells without activating agents, Carbon 41(4) (2003) 861–863.

[16] B. Al-Duri, K. Khader, G. McKay, Prediction of binary compound isotherm for adsorption on heterogeneous surfaces, J. Chem. Technol. Biotechnol. 53(4) (1992) 345–352.

[17] C. Theivarasu, S. Chandra, Preparation and characterisation of elephant dung activated carbon and its application for Rhodamine B adsorption, Orient. J. Chem. 27(2) (2011) 573–585.

[18] American Public Health Association Publications, Standard Methods for the Examination of Water and Wastewater, eighteenth ed., Greenberg, Washington, DC, 1992.

[19] R. Srivastsava, D.C. Rupainwar, A comparative evaluation for adsorption of dye on neem bark and mango bark powder, Indian J. Chem. Technol. 18(1) (2011) 67–75.

[20] M. Sarioglu, U.A. Atay, Removal of methylene blue by using biosolid, Global Nest J. 8(2) (2006) 113–120.

[21] A. Ozer, G. Akkaya, Removal of Acid Red 274 from wastewater: combined biosorption and biocoagulation with *Spirogyra Rhizopus*, Dyes Pigm. 71(2) (2006) 83–89.

[22] C. Namasivayam, N. Muniasamy, K. Gayatri, M. Rani, K. Ranganathan, Removal of dyes from aqueous solutions by cellulosic waste orange peel, Bioresour. Technol. 57(1) (1996) 37–43.

[23] Y.S. Ho, G. McKay, The sorption of lead (II) ions on peat, Water Res. 33(2) (1999) 578–584.

[24] S. Lagergren, About the theory of so-called adsorption of soluble substances, Kungliga Svenska Vetenskapsakdemiens Handlingar 24 (1898) 1–39.

[25] Y.S. Ho, G. McKay, The kinetics of sorption of divalent metal ions onto sphagnum moss peat, Water Res. 34(3) (2000) 735–742.

[26] A.B. Perez-Marin, V.M. Zapata, J.F. Ortuno, M. Aguilar, J. Saez, M. Lorens, Removal of cadmium form aqueous solutions by adsorption onto orange waste, J. Hazard. Mater. B139(1) (2007) 122–131.

[27] S.H. Chien, W.R. Clayton, Application of Elovich equation to the kinetics of phosphate release and sorption in soils, Soil Sci. Soc. Am. J. 44(2) (1980) 265–268.

[28] S. Idris, Y.A. Iyaka, B.E.N. Dauda, M.M. Ndamitso, M.T. Umar, Kinetic study of utilizing groundnut shell as an adsorbent in removing chromium and nickel from dye effluent, Am. Chem. Sci. J. 2(1) (2012) 12–24.

[29] B.H. Hameed, A.T.M. Din, A.L. Ahmad, Adsorption of methylene blue onto bamboo-based activated carbon: kinetics and equilibrium studies, J. Hazard. Mater. 141(3) (2007) 819–825.

[30] P.K. Malik, Dye removal from wastewater using activated carbon developed from sawdust: adsorption equilibrium and kinetics, J. Hazard. Mater. 113(1–3) (2004) 81–88.

[31] C. Namasivayam, D. Kavitha, Removal of Congo red from water by adsorption onto activated carbon prepared from coir pith, an agricultural solid waste, Dyes Pigm. 54(1) (2002) 47–58.

[32] V.S. Mane, I.D. Mall, V.C. Srivastava, Use of bagasse fly ash as an adsorbent for the removal of brilliant green dye from aqueous solution, Dyes Pigm. 73(3) (2007) 269–278.

[33] V. Vadivelan, K. Vasanthakumar, Equilibrium, kinetics, mechanism and process design for the sorption of methylene blue onto rice husk, J. Colloid Interf. Sci. 286(1) (2005) 90–100.

[34] M.S. Chiou, H.Y. Li, Adsorption behavior of reactive dye in aqueous solution on chemical cross-linked chitosan beads, Chemosphere 50(8) (2003) 1095–1105.

[35] G. Sreelatha, V. Ageetha, J. Parmar, P. Padmaja, Equilibrium and kinetic studies on reactive dye adsorption using palm shell powder (an agrowaste) and chitosan, J. Chem. Eng. Data 56(1) (2011) 35–42.

[36] M.C. Nicibi, B. Mahjoub, M. Seffen, Adsorptive removal of textile reactive dye using *Posidonia oceanica* (L.) fibrous biomass, Int. J. Environ. Sci. Tech. 4(4) (2007) 433–440.

[37] G. Crini, Non-conventional low-cost adsorbents for dyes removal: a review, Bioresour. Technol. 97(9) (2006) 1061–1085.

[38] R. Baseri, P.N. Palanisamy, P. Sivakumar, Adsorption of reactive dye by a novel activated carbon prepared from *Thevetia peruviana*, Int. J. Chem. Res. 3(2) (2012) 36–41.

[39] K.G. Bhattacharya, A. Sharma, Kinetics and thermodynamics of methylene blue adsorption on neem (*Azadirachta indica*) leaf powder, Dyes Pigm. 65(1) (2005) 51–59.

[40] C. Namasivayam, R.T. Yamuna, Adsorption of chromium (VI) by a low cost adsorbent: biogas residual slurry, Chemosphere 30(3) (1995) 561–578.

[41] E.E. El Katori, A.S. Fouda, A.A. Al-Sarawy, Removal of some thiazole dyestuffs from aqueous media by adsorption onto different types of carbon, Indian J. Chem. Technol. 18(4) (2011) 319–326.

[42] H.K. Boparai, M. Joseph, D.M. O'Carroll, Kinetics and thermodynamics of cadmium ion removal by adsorption onto nano zerovalent iron particles, J. Hazard. Mater. 186(1) (2011) 458–465.

[43] S. Senthilkumaar, S.K. Krishna, P. Kalamani, C.V. Subburaam, N. Ganapathi Subramaniam, Adsorption of organophosphorous pesticide from aqueous solution using "waste" jute fiber carbon, Mod. Appl. Sci. 4(6) (2010) 67–83.

[44] S. Goswami, U.C. Ghosh, Studies on adsorption behavior of Cr (VI) onto hydrous stannic oxide, Water SA 31(4) (2005) 597–602.

[45] W.J. Weber, J.C. Morris, Kinetics of adsorption on carbon from solution, J. Sanit. Eng. Div. Am. Soc. Civ. Eng. 89 (1963) 31–60.

[46] K. Vijayaragahvan, M.H. Han, S.B. Choi, Y.S. Yun, Biosorption of Reactive Black 5 by *Cornybacterium glutamicum* biomass immobilized in alginate and polysulfone matrices, Chemosphere 68(10) (2007) 1838–1845.

[47] G.E. Boyd, A.W. Adamson, L.S. Meyers, Jr. The exchange adsorption of ions from aqueous solutions by organic zeolite II: Kinetics, J. Am. Chem. Soc. 69(11) (1947) 2836–2848.

[48] X. Chun-hua, Y. Cai-ping, W. Xiang-mei, Adsorption of rhenium (VII) on amino-1,2,4-triazole resin [J], Hydrometallurgy 90(2–4) (2008) 221–226.

[49] J.I. Cortina, N. Miralles, Kinetic studies on heavy metal ions removal by impregnated resins containing di-(2,4,4 trymethylpentyl) phosphoric acid, Sol. Extract. Ion. Exch. 15(6) (1997) 1067–1074.

[50] F.E. Okieimen, F. Orhorhoro, Binding cadmium and copper ions with chemically modified cellulosic materials, Int. J. Environ. Anal. Chem. 24(4) (1986) 319–325.

[51] D. Reichenberg, Properties of ion exchange resins in relation to their structure. III. Kinetics of exchange, J. Am. Chem. Soc. 75(3) (1953) 589–597.

[52] C. Raji, T.S. Anirudhan, Chromium (VI) adsorption by sawdust carbon: kinetics and equilibrium, Indian J. Chem. Technol. 4(5) (1997) 228–236.

[53] N. Kannan, M. Sundaram, Kinetics and mechanism of removal of methylene blue by adsorption on various carbons-a comparative study, Dyes Pigm. 51(1) (2001) 25–40.

[54] S.Y. Wong, Y.P. Tan, A.H. Abdullah, S.T. Ong, Removal of Basic Blue 3 and Reactive Orange 16 by adsorption onto quartenized sugar cane bagasse, Malasian J. Analyt. Sci. 13(2) (2009) 185–193.

[55] S.W. Won, S.B. Choi, B.W. Chung, D. Park, J.M. Park, Y.S. Yun, Biosorptive decolourisation of Reactive Orange 16 using the waste biomass of *Corynebacterium glutamicum*, Ind. Eng. Chem. Res. 43(24) (2004) 7865–7869.

[56] W. Yue-zhong, L. Wen-qi, F. Zhao-hua, L. Wei-ping, Effects of adsorption interferents on removal of Reactive Red 195 dye in wastewater by chitosan, J. Environ. Sci. 17(5) (2005) 766–769.

[57] S. Wang, Y. Boyjoo, A. Choueib, Comparative study of dye removal using fly ash treated by different methods, Chemosphere 60(10) (2005) 1401–1407.

[58] N. Kamal Amin, Removal of reactive dye from aqueous solutions by adsorption onto activated carbons prepared from sugarcane bagasse pith, Desalination 223(1–3) (2008) 152–161.

[59] J. Monika, V. Garg, K. Kadirvelu, Chromium (VI) removal from aqueous solution, using sunflower stem waste, J. Hazard. Mater. 162(1) (2009) 365–372.

[60] Y.J. Li, B.Y. Gao, T. Wu, B. Wang, X. Li, Adsorption properties of aluminium magnesium mixed hydroxide for the model anionic dye Reactive Brilliant Red K-2BP, J. Hazard. Mater. 164(2–3) (2009) 1098–1104.

[61] S. Hashemian, S. Dadfarnia, M.R. Nateghi, F. Gafoori, Sorption of Acid Red 138 from aqueous solution into rice bran, Afr. J. Biotechnol. 7(5) (2008) 600–605.

[62] M. Ozacar, A. Sengil, Adsorption of acid dyes from aqueous solutions by calcined alunite and granular activated carbon, Adsorption 8(4) (2002) 301–308.

[63] P.N. Palanisamy, P. Sivakumar, Kinetic isotherm studies of the adsorption of Acid Blue 92 using low-cost non-conventional activated carbon, Desalination 249(1) (2009) 388–397.

[64] K. Kadirvelu, C. Karthika, N. Vennilamani, S. Pattabhi, Activated carbon from industrial solid waste as an adsorbent for the removal of Rhodamine B from aqueous solution: kinetic and equilibrium studies, Chemosphere 60(8) (2005) 1009–1017.

[65] H. Lata, V.K. Garg, R.K. Gupta, Adsorptive removal of basic dye by chemically activated *Parthenium* biomass: equilibrium and kinetic modeling, Desalination 219(1–3) (2008) 250–261.

[66] S. Arivoli, M. Thenkuzhali, M. Deva Prasath, Adsorption of Rhodamine B by acid activated carbon-kinetic, thermodynamic and equilibrium studies, Orient. J. Chem. 1(2) (2009) 138–155.

[67] S. Madhavakrishnan, K. Manickavasagam, R. Vasanthakumar, K. Rasappan, R. Mohanraj, S. Pattabhi, Adsorption of crystal violet dye from aqueous solution using *Ricinus Communis* pericarp carbon as adsorbent, E-J. Chem. 6(4) (2009) 1109–1116.

[68] D. Mohan, K.P. Singh, G. Singh, K. Kumar, Removal of dyes from wastewater using flyash, a low-cost adsorbent, Ind. Eng. Chem. Res. 41(15) (2002) 3688–3695.

[69] M. Hema, S. Arivoli, Adsorption kinetics and thermodynamics of malachite green dye onto acid activated low cost carbon, J. Appl. Sci. Environ. Manage. 12(1) (2008) 43–51.

[70] C. Jindarom, V. Meeyoo, T. Rirksomboon, P. Rangsunvigit, Thermochemical decomposition of sewage sludge in CO_2 and N_2 atmosphere, Chemosphere 67(8) (2007) 1477–1484.

[71] C. Theivarasu, S. Chandra, Removal of malachite green from aqueous solution by elephant dung activated carbon: kinetic, thermodynamic and isotherm studies, Indian J. Environ. Prot. 32(3) (2012) 215–223.

[72] C. Theivarasu, S. Chandra, Preparation and characterization of elephant dung activated carbon and its application as biosorbent for the removal of Reactive Orange 16 from aqueous solution, Electron. J. Environ., Agric. Food Chem. 10(8) (2011) 2783–2797.

[73] H.M.F. Freundlich, Over the adsorption in solution, J. Phys. Chem. 57A (1906) 385–470.

[74] F. Colak, N. Atar, A. Olgun, Biosorption of acidic dyes from aqueous solution by *Paenibacillus macerans*: kinetics, thermodynamic and equilibrium studies, Chem. Eng. J. 150(1) (2009) 122–130.

[75] K.K.H. Choy, G. McKay, J.F. Porter, Sorption of acid dyes from effluents using activated carbon, Resour. Conserv. Recycl. 27(1) (1999) 57–71.

[76] Z. Zaman Chowdhury, S. Mohd. Zain, R. Atta Khan, M. Aqeel Ashraf, Preparation, characterization and adsorption performance of the KOH-activated carbons derived from kenaf fiber for lead (II) removal from waste water, Sci. Res. Essays 6(29) (2011) 6185–6196.

[77] S. Saxena, P. Shrivastava, Ground water quality of a typical urban settlement, a case study of impact of town planning, Pollut. Res. 21(2) (2002) 223–226.

[78] P. Nagarajan, T.R. Moorthy, R.E. Raja, A.P. Raj, Physicochemical characteristics of water and soil at Senthanipuram, Trichirapalli and their influence on germination on green gram and cowpea, J. Ecotoxicol. Environ. Monitor. 15(3) (2005) 229–234.

[79] S. Umamahehwari, Water quality assessment of river Thamirabarani at Ambasamudram, J. Ecotoxicol. Environ. Monitor. 14(4) (2004) 273–276.

[80] Y.M. Slokar, M. Le Marechal, Methods of decoloration of textile waste waters, Dyes Pigm. 37(4) (1998) 335–356.